Available online at www.sciencedirect.com
ScienceDirect
Journal of Power Sources 180 (2008) 516–529
JOURNAL OF POWER SOURCES
www.elsevier.com/locate/jpowsour

# Hydrogen production by reforming of liquid hydrocarbons in a membrane reactor for portable power generation—Model simulations

Ashok S. Damle *

*RTI International, P.O. Box 12194, Research Triangle Park, NC 27709, USA*

Received 29 November 2007; received in revised form 29 January 2008; accepted 29 January 2008
Available online 7 February 2008

**Abstract**

One of the most promising technologies for lightweight, compact, portable power generation is proton exchange membrane (PEM) fuel cells. PEM fuel cells, however, require a source of pure hydrogen. Steam reforming of hydrocarbons in an integrated membrane reactor has potential to provide pure hydrogen in a compact system. In a membrane reactor process, the thermal energy needed for the endothermic hydrocarbon reforming may be provided by combustion of the membrane reject gas. The energy efficiency of the overall hydrogen generation is maximized by controlling the hydrogen product yield such that the heat value of the membrane reject gas is sufficient to provide all of the heat necessary for the integrated process. Optimization of the system temperature, pressure and operating parameters such as net hydrogen recovery is necessary to realize an efficient integrated membrane reformer suitable for compact portable hydrogen generation. This paper presents results of theoretical model simulations of the integrated membrane reformer concept elucidating the effect of operating parameters on the extent of fuel conversion to hydrogen and hydrogen product yield. Model simulations indicate that the net possible hydrogen product yield is strongly influenced by the efficiency of heat recovery from the combustion of membrane reject gas and from the hot exhaust gases. When butane is used as a fuel, a net hydrogen recovery of 68% of that stoichiometrically possible may be achieved with membrane reformer operation at 600 °C (873 K) temperature and 100 psig (0.791 MPa) pressure provided 90% of available combustion and exhaust gas heat is recovered. Operation at a greater pressure or temperature provides a marginal improvement in the performance whereas operation at a significantly lower temperature or pressure will not be able to achieve the optimal hydrogen yield. Slightly higher, up to 76%, net hydrogen recovery is possible when methanol is used as a fuel due to the lower heat requirement for methanol reforming reaction, with membrane reformer operation at 600 °C (873 K) temperature and 150 psig (1.136 MPa) pressure provided 90% of available combustion and exhaust gas heat is recovered.


*Keywords:* Hydrogen; Membrane; Reforming; Portable; Integrated; Compact

## 1. Background

One of the most promising technologies for lightweight portable power generation is proton exchange membrane (PEM) fuel cell. PEM fuel cells have several attractive features for small portable power applications: compact size, high power density, rapid start-up, and high energy conversion efficiency. Alternative technologies such as solid oxide fuel cells require very high temperatures of the order of 800–900 °C (1073–1173 K) for successful operation and also need much longer start-up time. PEM fuel cells have a potential to provide compact high energy density portable power, from a few Watts to a few kilo-Watts, both in consumer industry as well as in military applications. Consumer applications range from back-up premium power, battery charger, recreational power, e.g. camping, and emergency power. Military applications include lighter and more compact electrical power sources for soldier and robotic missions; and as the available technologies and instrumentation advance, so does the power requirement for equipment. For example, for the modern "land warrior," electrical energy is needed to power a variety of advanced devices such as a computerized radio system (transmission/receiver); helmet-mounted display, imager, and laser detector; and a weapon subsystem consisting of a laser rangefinder, thermal weapon sight, digital compass and a laser aiming

* Tel.: +1 919 541 6146; fax: +1 919 541 8002.
*E-mail address:* adamle@rti.org.

0378-7753/$ – see front matter © 2008 Elsevier B.V. All rights reserved.
doi:10.1016/j.jpowsour.2008.01.063

light. The desired amount of stored energy depends on application, with energy content of 1 kWh may be considered typical for emergency and backup power applications [1].

At present, batteries are used for powering such portable devices in military and consumer applications. Although batteries have many desirable features such as reliability, long storage life, air-independent operation, low thermal and acoustic signatures, etc., the amount of energy that can be stored in primary or rechargeable batteries is limited. Primary standard batteries such as BA5590 ($Li/SO_2$) have a specific energy of only 175 Wh $kg^{-1}$. The specific energy of the rechargeable secondary batteries under consideration by Army is even lower, for example specific energy of a BB2847 battery is about 80 Wh $kg^{-1}$ and that of a BB390A battery is only 56 Wh $kg^{-1}$. Consumer batteries have much lower energy densities, e.g. a high capacity lead acid battery provides an energy density of about 23 Wh $kg^{-1}$. While many improvements in battery technology are being made and future advances are anticipated, the projected specific energies are still expected to be substantially lower than the desired specific energies of 1000 Wh $kg^{-1}$ or greater.

Power densities of large 80–100 kW PEM systems being developed for automotive power application are greater than 0.6 kW $kg^{-1}$ and are approaching 1 kW $kg^{-1}$. For smaller, e.g. 20–100 W power systems, a fuel cell power density greater than at least 0.2 kW $kg^{-1}$ is expected. PEM fuel cells are therefore very attractive as a power generation unit for the small portable power generation systems. PEM fuel cells, however, require a source of pure hydrogen. Approaches available for supplying hydrogen to a fuel cell include compressed hydrogen cylinders, hydrogen adsorbed on metal hydrides, thermolysis or hydrolysis of metal hydrides, reforming of hydrocarbon fuels, and ammonia decomposition. With a typical 50% energy conversion efficiency of a fuel cell, about 17 kWh of electrical energy can be produced from 1 kg of hydrogen. To provide an energy capacity of 1 kWh, at least 0.06 kg of pure hydrogen must be provided. The commercially available choices for a hydrogen source are compared in Table 1 for their specific energies (electrical) based on the reagent weights alone.

As seen in Table 1, steam reforming of hydrocarbon fuels can provide reagent weight-based specific energies greater than 2000 Wh $kg^{-1}$ even after including weight of water. Butane and heavier hydrocarbons such as JP-8 indicate a high specific energy based on hydrocarbon fuel weight alone. However, for portable power applications the weight of water that is required for steam reforming must also be included in determining the overall specific energies of fuel/water mixture. The net specific energy of a hydrocarbon reforming system may be increased by recovering liquid water from the fuel cell exhaust gas and recycling it to the fuel reformer, however, it will need additional components and add complexity [2,3]. Although ammonia cracking can provide a high specific energy of 3000 Wh $kg^{-1}$, ammonia must be stored under pressure and is also considered toxic for portable use. Hydrocarbon fuels possess desirable characteristics such as ease of fuel storage at low pressures and ambient temperatures, handling and transportation; availability and a lower cost and would be considered as the primary candidates as hydrogen sources for fuel cell-based portable power.

Table 1
Hydrogen yield and corresponding specific energy (electrical) of fuel choices

| Fuel | Hydrogen yield, kg $kg^{-1}$ | Specific energy Wh $kg^{-1}$ |
|---|---|---|
| Compressed hydrogen[a] | 0.01 | 150 |
| Metal hydrides for storage[a] | 0.013 | 200 |
| $NaBH_4$ hydrolysis | 0.108 | 1830 |
| Methanol | 0.188 | 3190 |
| Methanol (including water) | 0.120 | 2040 |
| Butane | 0.448 | 7620 |
| Butane (including water) | 0.129 | 2190 |
| Gasoline | 0.444 | 7500 |
| Gasoline (including water) | 0.125 | 2140 |
| JP-8 | 0.435 | 7400 |
| JP-8 (including water) | 0.123 | 2090 |
| Clearlite[b] | 0.430 | 7350 |
| Clearlite (including water) | 0.120 | 2050 |
| Ammonia | 0.176 | 3000 |

[a] System-based values for commercially available small systems.
[b] A sulfur-free kerosene available commercially.
Note that the hydrogen yield and specific energy values for compressed hydrogen cylinders and metal hydride-based canisters are based on actual commercially available systems. Hydrogen yield and energy capacities for sodium borohydride hydrolysis and ammonia cracking are based on stoichiometric reactions and are based on the amount of reagents required. The hydrogen yield and energy capacity for methanol is based on its complete decomposition and subsequent stoichiometric water gas shift (WGS) reaction. Hydrogen yield and energy capacities for the hydrocarbons are based on steam reforming and subsequent WGS reaction with 100% conversion and assume a stoichiometric steam to carbon ratio of 2. The hydrocarbons noted are those readily available as liquid commercial fuels.

## 2. Steam reforming of hydrocarbon fuels

Steam reforming of methane and petroleum feedstocks, e.g. naphtha, is an industry standard process for generating hydrogen commercially and extensive information is available on thermodynamics, kinetics, and catalysis of the reforming reactions (e.g. [4]). Steam reforming of hydrocarbons in general is a metal-catalyzed reaction described by three stoichiometric reactions. First the hydrocarbon dissociates on the metal surface, and the hydrocarbon fragments react with adsorbed steam to produce CO and $H_2$:

$$C_nH_m + nH_2O \rightarrow nCO + (n + m/2)H_2$$
$$(\text{for } C_4H_{10}:\ \Delta H^\circ_{298} = +582.4\,\text{kJ mol}^{-1};$$
$$\text{for } C_8H_{18}:\ \Delta H^\circ_{298} = +1300\,\text{kJ mol}^{-1}) \quad (1)$$

The CO and $H_2$ produced by reaction (1) further undergo methanation and water gas shift (WGS) reactions to establish equilibrium concentrations of CO, $H_2$, $CH_4$, $CO_2$, and $H_2O$:

$$CO + 3H_2 \Leftrightarrow CH_4 + H_2O\,(\Delta H^\circ_{298} = -206\,\text{kJ mol}^{-1}) \quad (2)$$

$$CO + H_2O \Leftrightarrow CO_2 + H_2\,(\Delta H^\circ_{298} = -41.2\,\text{kJ mol}^{-1}) \quad (3)$$

While reaction (1) is strongly endothermic, the overall heat of reaction may be positive or negative, depending upon process conditions; most typically it is strongly endothermic, and heat must be supplied to the reformer, usually by burning part of the fuel. In a partial oxidation or also termed as autothermal reformer

process fuel combustion and subsequent steam reforming of the remaining fuel is conducted in a single reactor. Since air is often used in an autothermal reactor the resulting reformate gas contain much lower concentration of hydrogen than that would be generated by steam reforming of hydrocarbons [5]. This paper addresses the possible utilization of steam reforming of liquid hydrocarbons for providing hydrogen for portable, small, power generation systems. Fuel processors utilizing steam reforming of hydrocarbons are actively being developed for small and micro-scale portable hydrogen generators [3,6,7].

The desired overall hydrocarbon steam reforming reaction, with the stoichiometric steam to carbon ratio of 2 and maximum 100% yield of hydrogen, is represented as

$$C_nH_m + 2nH_2O \Leftrightarrow nCO_2 + (2n + m/2)H_2 \quad (4)$$

The actual proportion of various species ($H_2$, CO, $CH_4$, $CO_2$, and $H_2O$) in the reformate gas at equilibrium depends upon the process temperature and pressure conditions and the steam to carbon ratio used. Conventionally, the fuel reforming process is followed by a separate lower temperature WGS reaction step to increase hydrogen concentration in the product gas. For small portable power systems it would obviously be desirable to generate hydrogen in a single reactor, as considered here, without inter-step cooling.

To overcome the equilibrium limitations of the reforming and WGS reactions, it is customary to use a significant excess of steam in the reforming process to increase the yield of hydrogen. Excess steam is also often considered as a necessity to prevent carbon formation in the reforming process causing deactivation of the catalyst. However, an excess use of steam also causes significant reduction in the reagent weight-based hydrogen yield. For example, stoichiometric steam reforming of butane will produce a maximum of 0.129 kg $H_2$ $kg^{-1}$ of reagents (Table 1) representing ~2200 Wh $kg^{-1}$ of specific energy (electrical) based on reagent weight alone. With 100% excess steam, however, the maximum hydrogen yield would be reduced to 0.075 kg $kg^{-1}$ of reagents representing only ~1280 Wh $kg^{-1}$ of specific energy (electrical) based on weight of reagents alone. The specific energy may be increased by condensing and recycling the excess water, however, the recovery is not usually complete and additional energy must be spent in vaporizing the excess water. Greater feed flow rates also increase the size and weight of the reactor and auxiliary systems. For generation of pure hydrogen, even greater excess of steam with steam to carbon ratio of greater than 4 is used in commercial practice. To increase the equilibrium conversion in the hydrocarbon reforming step high temperatures of 800 °C (1073 K) or more are also commercially used [4].

## 3. Membrane reactor concept

Another way of overcoming the equilibrium limitations as well as of reducing reactor temperatures to milder 500–600 °C (773–873 K) conditions, is to continuously separate the product hydrogen from the reaction mixture forcing the reforming reaction to go forward. For such a concept, a high-flux, high selectivity membrane stable at the reforming conditions is needed. Since the palladium-based hydrogen separation membranes also operate best at the target reforming conditions of 500–600 °C (773–873 K), have high flux rates, and are completely selective for hydrogen, these membranes are promising candidates for the membrane reactor/reformer concept. In membrane reforming process steam to carbon ratio can also be significantly lower than in a conventional reforming process since the hydrogen separation drives the equilibrium towards continued hydrogen generation. Stoichiometric utilization of steam will reduce the weight of reagents as well as the weight and size of the overall system and will allow realization of the high specific energies noted in Table 1. Utilization of a high-selectivity hydrogen separation membrane also provides a purer hydrogen product stream and will reduce any additional purification needed to produce hydrogen product suitable for use in a PEM fuel cell.

In order to realize a high specific energy for the overall reforming process unit, heat must be supplied to the process efficiently while minimizing heat losses. For maximizing thermal energy utilization it is desirable to integrate the generation of heat by fuel combustion with the utilization of heat by the reforming reaction as shown schematically in an integrated "membrane reactor" configuration (Fig. 1). Such configuration may be realized in a planar geometry or in a concentric tubular geometry where the heat transfer surface separates a heat generation (fuel combustion) section from the hydrocarbon reformer section. The heat transfer surfaces in Fig. 1 are indicated as mesochannel in reference to a possible miniature planar geometry design where the flow channels are etched as grooves on the surface. Several alternative designs are of course possible for example catalyst incorporated in a porous foam structure.

In the combustor section an auxiliary fuel is burned to produce heat. As seen in Fig. 1 schematic, the heat value of the residual

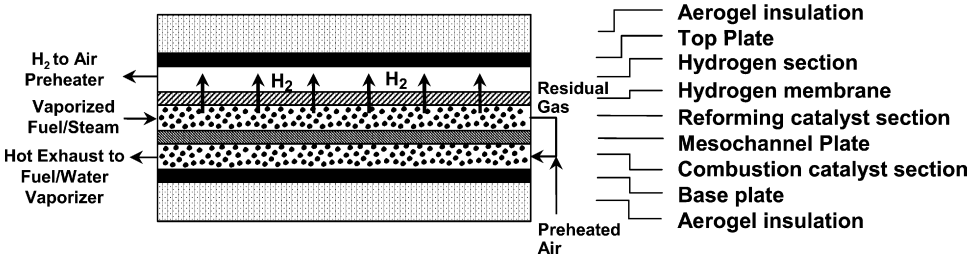


Fig. 1. Schematic of an integrated membrane reactor.

gas leaving the membrane reformer section can be used in the combustor section along with any fuel cell anode exhaust gas to minimize or preferably eliminate the auxiliary fuel requirement. To further improve thermal efficiency of the overall system, the heat from the combustor exhaust gases and the hydrogen product may be recovered to preheat the air used for the combustor and to heat/vaporize fuel/water mixture. Furthermore, the heat losses from the system should also be minimized by enclosing the system in an efficient insulation material.

Numerous studies have been conducted for evaluation of the membrane reactor concept for conducting steam methane reforming (SMR) and WGS reactions [8–12]. Palladium alloy foils or tubes have also been incorporated in small hydrocarbon fuel reformers that are being demonstrated (e.g. [13–15]). Palladium alloy membranes are used either to purify the product hydrogen after a fuel reformer [13,14] or integrated within the fuel reforming process [15] as shown in Fig. 1 schematic. This paper presents the results of model simulations conducted for evaluation of the membrane reactor concept for reforming liquid hydrocarbon fuels, butane and methanol. In a companion paper, experimental results obtained for reforming butane, methanol as well as clearlite (a sulfur-free kerosene available commercially) fuels in a palladium-based membrane reactor are compared with model predictions. These fuels are selected because of their commercial availability and varying degree of difficulty anticipated in reforming hydrocarbon fuels. Steam reforming of butane and clearlite occurs as described by Eqs. (1)–(4) discussed above. Methanol on the other hand decomposes readily at temperatures above 300 °C (573 K) in an endothermic reaction [9]:

$$CH_3OH \Leftrightarrow 2H_2 + CO \,(\Delta H^\circ_{298} = +100.5\,\text{kJ mol}^{-1}) \quad (5)$$

With the subsequent exothermic and equilibrium limited WGS reaction (reaction (3)) the overall steam reforming of methanol is described as

$$CH_3OH + H_2O \Leftrightarrow 3H_2 + CO_2$$
$$(\Delta H^\circ_{298} = +59.3\,\text{kJ mol}^{-1}) \quad (6)$$

Enhancement of equilibrium conversion through separation of one of the products by a membrane is not a new concept; and a number of studies have confirmed the merits of the membrane reactor approach [16,17]. Several attempts to use the product permeation concept in reactor technology have emerged through the years. Removing hydrogen product through a palladium membrane tube has also been proposed for the promotion of the dehydrogenation reaction of cyclohexane to benzene beyond thermodynamic equilibrium [18,19]. A reaction conversion of 99.7% was reported compared to 18.7% using an ordinary catalytic reactor. Different types of ceramic membranes have also been investigated as $H_2$ permeators. A sol–gel alumina membrane was utilized in a ceramic tubular reactor for propane dehydrogenation [20].

In addition to continuous shifting of the reaction equilibrium driving it to completion, the use of a membrane reactor would also allow using lower temperatures (600 °C (873 K) and lower) for the reforming reaction. Steam methane reforming reaction (reaction (2)) is favored at a higher temperature (>700 °C (>973 K)) and a lower pressure to produce increased hydrogen. However, greater conversions are possible at lower temperatures and higher pressures in a membrane reactor since the separation of one of the product species ($H_2$) overcomes the thermodynamic limitations of the reaction. It also permits the use of a smaller reactor and separator, and allows operation at a greater residence time. The benefit is decreased reactor cost (cheaper materials, smaller vessel, and less catalyst), fewer side reactions and improved heat transfer. The WGS shift reaction on the other hand is favored at temperatures below 400 °C (673 K) for increased hydrogen. However, again separation of hydrogen product allows conducting WGS reaction at a much higher temperature of 600 °C (873 K) by shifting the WGS reaction equilibrium. The membrane reactor–steam reformer unit can also conduct both the steam reforming and the subsequent WGS reaction in a single reactor by continuing them simultaneously. Another advantage of the membrane reactor concept is that a large excess of steam to carbon ratio is not necessary for achieving equilibrium. Stoichiometric steam to carbon ratio can be used in the membrane reactor configuration by utilizing appropriate catalysts (e.g. precious metal-based catalysts) resistant to carbon formation.

### 3.1. Membrane reactor model development

To determine the potential benefits of the membrane reactor concept for hydrogen generation by liquid hydrocarbon fuel reforming in small, portable integrated systems, a simple, one-dimensional membrane reactor model was developed taking into account the effect of hydrogen permeation on equilibrium composition of the reacting species. The membrane reactor model and computation methodology was originally developed for simultaneous hydrogen separation and WGS reaction [21] and is modified here to include both the methane reforming equilibrium along with the WGS reaction equilibrium. The simulated one-dimensional membrane reactor is shown schematically in Fig. 2a. The basic assumptions of this simple model are [21]:

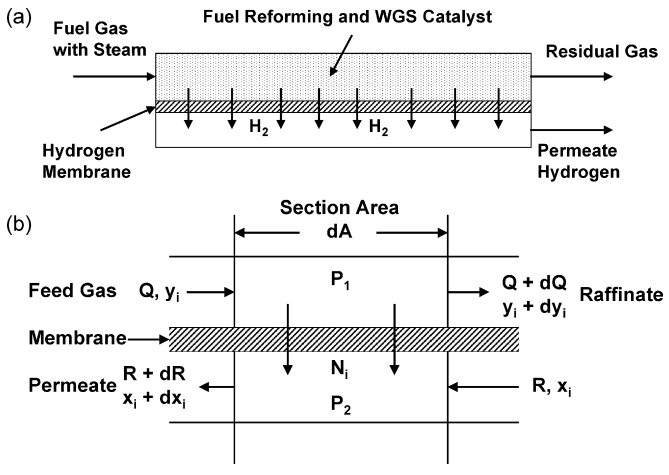


Fig. 2. (a) Membrane reactor schematic. (b) Schematic of a membrane reactor section.

- membrane reactor temperature is the same and constant along the length of the reactor on both permeate and feed sides,
- the total pressures on feed and permeate sides remain constant along the length of the reactor, i.e. there is no pressure drop along the length on either side,
- hydrogen flux at any location along the length of the membrane reactor is determined by the local driving force, i.e. partial pressure differential across the membrane,
- permeation of all other species is determined by membrane species selectivity for hydrogen with respect to each species as provided,
- both the methane reforming (methanation) as well as the WGS reactions (reactions (2) and (3)) are taken into account to determine equilibrium composition on the feed side after incremental hydrogen permeation along the length of the membrane reactor,
- Reaction kinetics for all reactions is assumed fast enough allowing the feed side gas composition to be in dynamic equilibrium along the length of the membrane reactor.
- no reactions occur on the permeate side, and
- no sweep gas is used on the permeate side.

This simple model assumes dynamic equilibrium composition on the feed side including that at the feed inlet position. This in effect assumes that the membrane reactor follows a pre-reformer where the fuel–steam mixture is brought to an equilibrium composition as a result of complete reforming of fuel by reactions (1) (or (5) for methanol) followed by simultaneous equilibrium reactions (2) and (3) at the membrane reactor operating conditions of temperature and pressure. The membrane reactor area is divided in a large number of increments with user-defined incremental permeation for each increment. Relative permeation of all other species is determined from user provided species selectivity correlations.

The reaction and mass transfer processes occurring in an area increment are shown schematically in Fig. 2b of a section of a membrane reactor of surface area $dA$, $m^2$. The pressures on the feed and permeate sides are assumed to be constant, $P_1$ (Pa) and $P_2$ (Pa), respectively. $Q$ (mol $s^{-1}$) is the molar feed gas flow entering the reactor section with $y_i$ the mole fraction of component $i$. $R$ (mol $s^{-1}$) is the molar flow of permeate entering the reactor with $x_i$ the mole fraction of component $i$. $dQ$, $dR$ are molar flow rate changes in the reactor section and $dy_i$ and $dx_i$ are respective mole fraction changes for component $i$. $N_i$ (mol $s^{-1}$) is the molar flow of component $i$ across the membrane. The feed and permeate flows are shown counter-current to each other in the flow scheme; however, rate relations are developed here for both the con-current and counter-current flow schemes.

The molar flow, $N_i$ (mol $s^{-1}$) of component $i$ across the membrane is expressed by a general power law correlation:

$$N_i = (P_1^z y_i^z - P_2^z x_i^z) K_1 \alpha_{i,1}\, dA \tag{7}$$

where $z$ is the power law exponent for the permeability correlation that depends on the mechanism for the component permeation, $K_1$ is the permeability coefficient of reference component 1 in mol $m^{-2}$ $s^{-1}$ $Pa^{-z}$, and $\alpha_{i,1}$ is the permeability ratio of component $i$ with respect to component $1 = K_i/K_1$, and for linear dependency of the flux on the concentration driving force the power law exponent is 1. For diffusion of hydrogen through bulk (thick) palladium membrane the power law exponent is 0.5 according to Sievert's Law [22]. For thin palladium composite membranes, however, other factors such as gas phase mass transfer resistance also become important resulting in a higher exponent between 0.5 and 1 [23].

Defining a membrane pressure ratio $P_r = P_1/P_2$, the above equation is rewritten as

$$N_i = (P_r^z y_i^z - x_i^z) \alpha_{i,1} K_1 P_2^z\, dA \tag{8}$$

The changes in total molar flows through the reactor section, $dQ$ and $dR$ (mol $s^{-1}$), are given by adding fluxes for all components.

$$dQ = -dR = -\sum N_i \tag{9}$$

Substituting for $N_i$

$$\left(\frac{1}{K_1 P_2^z}\right)\frac{dQ}{dA} = \left(\frac{1}{K_1 P_2^z}\right)\frac{dR}{dA} = -\sum (P_r^z y_i^z - x_i^z)\alpha_{i,1} \tag{10}$$

(Note that in the feed flow direction $dQ/dA = dR/dA$).

Species mass balance for component $i$ across the feed side of the membrane reactor provides

$$Q_{y_i} = (Q + dQ)(y_i + dy_i) + N_i \tag{11}$$

Substituting for $dQ$ and $N_i$ and ignoring the second order terms

$$\left(\frac{1}{K_1 P_2^z}\right)\frac{dy_i}{dA} = \left(\frac{y_i}{Q}\right)\left[\sum (P_r^z y_i^z - x_i^z)\alpha_{i,1}\right] - (P_r^z y_i^z - x_i^z)\frac{\alpha_{i,1}}{Q} \tag{12}$$

A similar component balance on the permeate side provides

$$\left(\frac{1}{K_1 P_2^z}\right)\frac{dx_i}{dA} = \left(\frac{x_i}{R}\right)\left[\sum (P_r^z y_i^z - x_i^z)\alpha_{i,1}\right] - (P_r^z y_i^z - x_i^z)\frac{\alpha_{i,1}}{R} \tag{13}$$

For a con-current flow scheme, the equations describing $dQ$ and $dy_i$ remain the same, and in equations describing $dR$ and $dx_i$, signs are reversed on the right side of the above equations, i.e.

$$\left(\frac{1}{K_1 P_2^z}\right)\frac{dR_i}{dA} = \left[\sum (P_r^z y_i^z - x_i^z)\alpha_{i,1}\right] \tag{14}$$

$$\left(\frac{1}{K_1 P_2^z}\right)\frac{dx_i}{dA} = -\left(\frac{x_i}{R}\right)\left[\sum (P_r^z y_i^z - x_i^z)\alpha_{i,1}\right] + (P_r^z y_i^z - x_i^z)\frac{\alpha_{i,1}}{R} \tag{15}$$

The model simulations use 1 mol $s^{-1}$ of feed gas of the initial feed gas composition as basis. Computations begin with calculation of equilibrium feed side gas composition for the

membrane reactor operating conditions of temperature, pressure and the feed gas composition provided. Species material balance equation for each species are solved over the area increment d$A$ corresponding to the specified incremental permeation and the change in gas compositions occurring as a result of permeation of all species through the membrane are determined for both the feed and permeate sides. The feed side gas composition and the molar flow rate are then updated for the next increment assuming simultaneous equilibrium for the methane reforming and WGS reactions (reactions (2) and (3)). For each increment, exit flow rates and compositions of both the feed side retentate and sweep side permeate gases, reaction conversion, hydrogen recovery, and incremental membrane area requirement for the incremental hydrogen permeation is calculated. Model computations then proceed to the next increment. The simulation is terminated when a pre-determined low enough hydrogen partial pressure differential across the membrane is reached, continued hydrogen permeation beyond which will require prohibitively large membrane areas for additional incremental hydrogen recovery. The equilibrium gas compositions are calculated using the equilibrium constants for the methane reforming (reverse methanation) and WGS reactions as

$$K_{\mathrm{WGS}} = y_{\mathrm{H_2}} y_{\mathrm{CO_2}} / y_{\mathrm{CO}} / y_{\mathrm{H_2O}} \quad (16)$$

$$K_{\mathrm{methanation}} = y_{\mathrm{CH_4}} y_{\mathrm{H_2O}} / y_{\mathrm{CO}} / y_{\mathrm{H_2}}^3 \quad (17)$$

where $y_i$ is the mole fraction of species $i$ in the feed gas. A chemical reaction and equilibrium software with extensive thermo-chemical database, "Outokumpu HSC Chemistry Software" HSC Chemistry 4.0 [24] is used to determine the WGS as well as methanation reaction equilibrium constants for the process conditions used in model simulations.

For a given steam to fuel carbon ratio, the initial feed gas composition for the membrane reactor model simulation is provided by assuming complete conversion in reaction (1) (reaction (5) for methanol reforming) followed by equilibrium conditions for both reactions (2) and (3) for the process conditions being simulated. It may be noted that the initial feed gas composition is quite similar for butane or any higher-carbon-number hydrocarbons in the homologus series ($C_nH_{2n+2}$) approximated for kerosene, JP-8 or clearlite as the fuel being reformed, e.g. for steam to carbon ratio of 2, the feed gas composition assuming complete conversion of reaction (1) for butane is: $H_2$:CO:$H_2O$: 2.25:1:1. For clearlite, assuming an equivalent molecular formula of $C_{12}H_{26}$ the feed gas composition would be approximately $H_2$:CO:$H_2O$: 2.083:1:1. For methanol (taking into account the presence of oxygen in the molecule and thus using steam to methanol ratio of 1) the feed gas composition would be $H_2$:CO:$H_2O$: 2:1:1, slightly different than that for butane. The model simulations were therefore conducted for butane and methanol as hydrocarbon fuels covering the range of commercially available hydrocarbon fuels.

Model simulations were conducted for steam reforming of butane, using feed side pressure, membrane reactor temperature, and steam to carbon ratio in the feed gas as process variables, to estimate increase in overall conversion to hydrogen and net hydrogen recovery as hydrogen is continuously permeated through the membrane along the length of a membrane reactor. Percentage conversion of the hydrocarbon to hydrogen is defined as the total amount of hydrogen produced (present in the feed side as well as the permeate side gas streams) compared to the maximum possible hydrogen generation potential including the WGS reaction. Net percentage hydrogen recovery is defined as the amount of product hydrogen separated in the permeate stream compared to the maximum possible hydrogen generation potential. The maximum hydrogen potential assumes complete conversion in the reforming and WGS reactions, i.e. that given by reaction (4). For example, for butane the maximum hydrogen potential is 13 moles of hydrogen per mole of butane in the feed gas. Although dense palladium is completely selective to hydrogen compared to other gases present in the reforming gas mixture, defects and pinholes present in the membrane often limits the practical selectivity of the membrane for hydrogen. In these simulations the hydrogen separation membrane is assumed to be highly selective for hydrogen with a perm-selectivity of 1000 for hydrogen compared to all other gas species.

## 4. Membrane reactor model simulations

### 4.1. Steam reforming of butane

Model simulations were conducted to predict increase in butane conversion to hydrogen as hydrogen is continuously separated from the feed side reaction mixture in the membrane reactor. The simulation parameters included membrane temperatures of 550, 600 and 650 °C (823, 873, and 923 K), steam to carbon ratio of 2, 3, and 4, and membrane pressure ratios of 5.1, 7.8, and 11.2 corresponding to feed side pressures of 60, 100, and 150 psig (0.515, 0.791, and 1.136 MPa) with permeate at atmospheric pressure. Figs. 3–5 indicate the predicted conversion of butane to hydrogen and net recovery of hydrogen in the permeate stream as a function of the amount of hydrogen permeated, in moles per mole of inlet feed gas, for steam reforming of butane conducted in a membrane reactor at 60, 100, and 150 psig (0.515, 0.791, and 1.136 MPa) system pressure, respec-

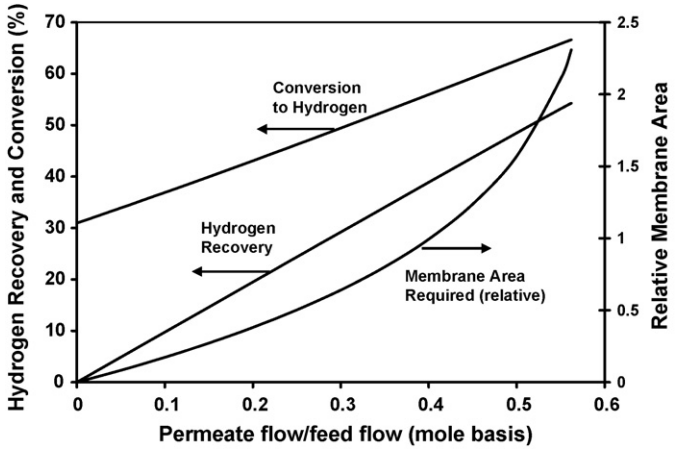


Fig. 3. Conversion of butane to hydrogen and net hydrogen recovery, at 873 K, 0.515 MPa feed side pressure, 0.101 MPa permeate side pressure, steam to carbon ratio 2.

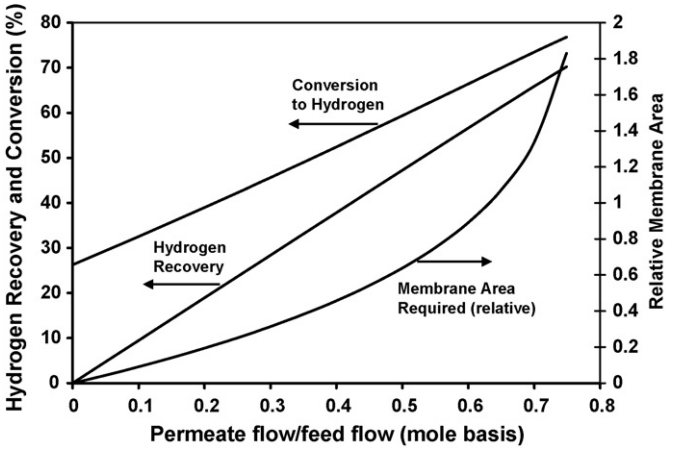


Fig. 4. Conversion of butane to hydrogen and net hydrogen recovery, at 873 K, 0.791 MPa feed side pressure, 0.101 MPa permeate side pressure, steam to carbon ratio 2.

tively, with permeate being at atmospheric pressure. The reactor temperature was held constant at 600 °C (873 K) and a steam to carbon ratio of 2.0 was used in these simulations. Operation at lower temperatures is likely to reduce hydrogen yield due to unfavorable methane reforming thermodynamics as well as slower reaction kinetics; and operation at higher temperatures will likely lead to materials/seals issues. Model simulations with the steam to carbon ratio of 2 correspond to stoichiometric utilization of steam, an important benefit of the membrane reactor concept. A linear dependency of the hydrogen flux on the concentration driving force was assumed in these model simulations with the power law exponent of 1 as observed for thin Pd film composite membranes. Figs. 3–5 also indicate the relative membrane area required as a function of the amount of hydrogen permeated. The actual membrane area required is determined using the hydrogen permeation characteristics of the membrane used.

These figures clearly indicate increased conversion of butane to hydrogen as hydrogen is continuously removed from the reacting gas mixture due to shift in the reaction equilibrium.

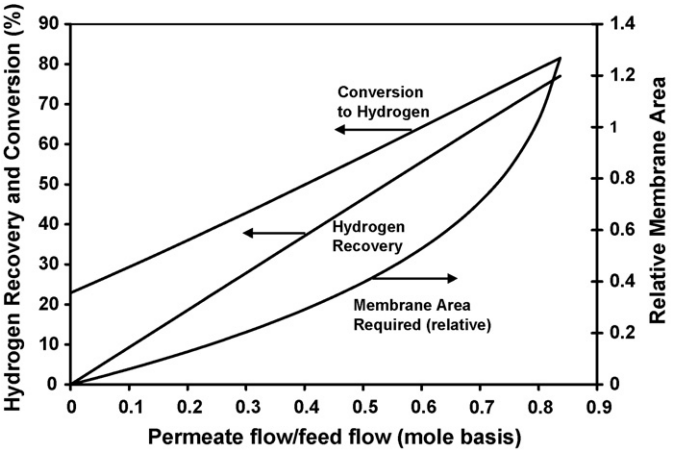


Fig. 5. Conversion of butane to hydrogen and net hydrogen recovery, at 873 K, 1.136 MPa feed side pressure, 0.101 MPa permeate side pressure, steam to carbon ratio 2.

The maximum possible recovery of hydrogen is limited by the requirement of maintaining positive hydrogen partial pressure differential across the membrane. Thus operation of the membrane reactor at greater feed side pressures obviously allows greater amount of hydrogen to permeate with greater hydrogen recovery as reflected in these simulations. The membrane area required for incremental hydrogen recovery increases as more and more hydrogen is permeated due to decreasing hydrogen partial pressure differentials across the membrane with increasing recovery of hydrogen. Thus incremental membrane area requirement increases dramatically at high hydrogen recoveries as expected.

These simulations indicate that progressively greater hydrogen conversions and recoveries are possible by operating the membrane reactor at a higher pressure. These model simulations assume dynamic feed side equilibrium with fast reaction kinetics. Although higher pressures are unfavorable for methane reforming reaction (reverse of reaction (2)) and high temperatures are unfavorable for WGS reaction (reaction (3)) the effect of high pressure and high temperature on reaction equilibriums is offset by continuous removal of hydrogen shifting the respective reaction equilibriums to more hydrogen conversion. The advantage of increasing the system pressure from 60 to 100 psig (0.515–0.791 MPa) appears to be more significant with a predicted increase in hydrogen recovery from 53 to 71%, than the increase in pressure from 100 to 150 psig (0.791–1.136 MPa) with a smaller improvement in hydrogen recovery from 71 to 77%.

The change in the residual feed side gas composition, as hydrogen is continuously permeated, is presented in Figs. 6 and 7 for the corresponding cases of butane reforming at 600 °C (873 K), steam to carbon ratio of 2, ambient permeate side pressure, and the feed side pressures of 100 and 150 psig (0.791 and 1.136 MPa), respectively. Membrane reactor operation at a higher pressure clearly results in greater $CO_2$ concentration and lower hydrogen concentration on the feed side of the membrane at the reactor exit as expected with greater conversion to hydrogen and hydrogen recovery at a higher pressure. Also greater initial methane formation is predicted at higher pressure membrane reactor operation to maintain methanation reaction equilibrium. The partial pressure of hydrogen at the

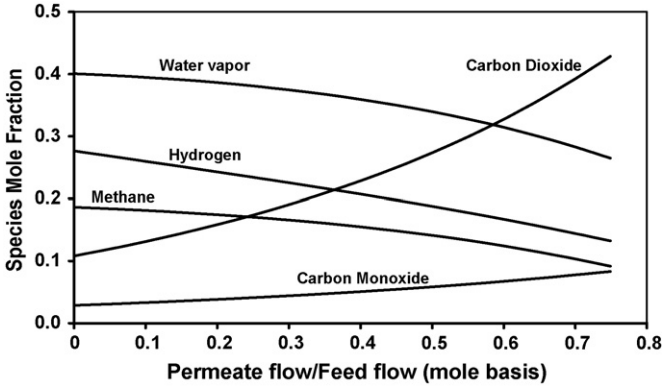


Fig. 6. Feed side gas composition, 873 K, 0.791 MPa feed side pressure, 0.101 MPa permeate side pressure, steam to carbon ratio 2.

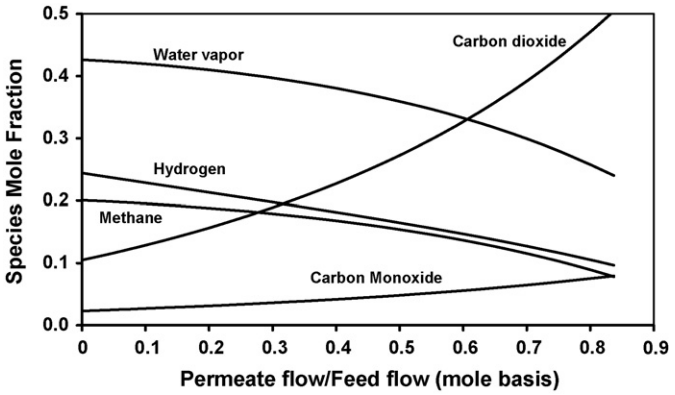


Fig. 7. Feed side gas composition, 873 K, 1.136 MPa feed side pressure, 0.101 MPa permeate side pressure, steam to carbon ratio 2.

exit of the membrane reactor approaches that in the permeate stream and model simulations are terminated when the partial pressure differential becomes quite small (less than 0.5 psia (0.0034 MPa)).

Although stoichiometric utilization of steam to carbon ratio is desirable, greater steam to carbon ratios are usually used especially to avoid carbon formation [4,25]. In conventional reforming operations steam to carbon ratio as high as 5–6 is often used to overcome the equilibrium limitations [4]. The effect of a greater steam to carbon ratios of 3 and 4 was therefore investigated by model simulations for process conditions of 600 °C (873 K) temperature, 100 psig (0.791 MPa) feed side pressure and 0 psig (0.101MPa) permeate side pressure and the results are shown in Figs. 8 and 9 for steam to carbon ratio of 3 and in Figs. 10 and 11 for steam to carbon ratio of 4. These results may be compared with simulation results shown in Figs. 4 and 6, respectively, for the steam to carbon ratio of 2. Comparison of Figs. 6, 9 and 11 indicates increased hydrogen concentration and reduced methane/CO concentrations due to greater amount of water reagent available in the feed gas at greater steam to carbon ratios. The conversion to hydrogen increased from 76 to 93% as seen from Figs. 4, 8 and 10. However, in spite of the significantly

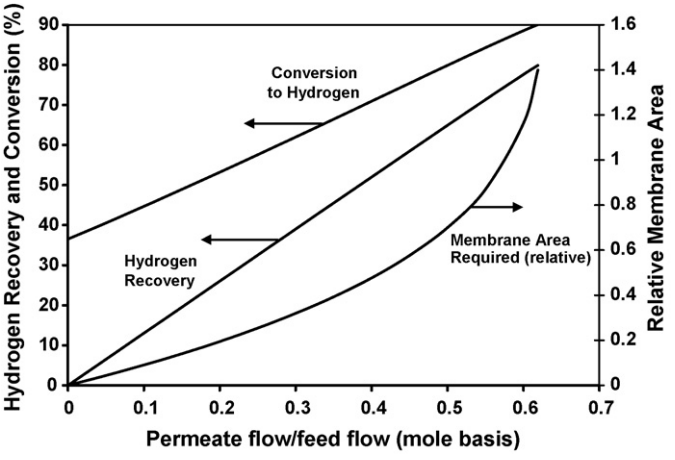


Fig. 8. Conversion of butane to hydrogen and net hydrogen recovery, at 873 K, 0.791 MPa feed side pressure, 0.101 MPa permeate side pressure, steam to carbon ratio 3.

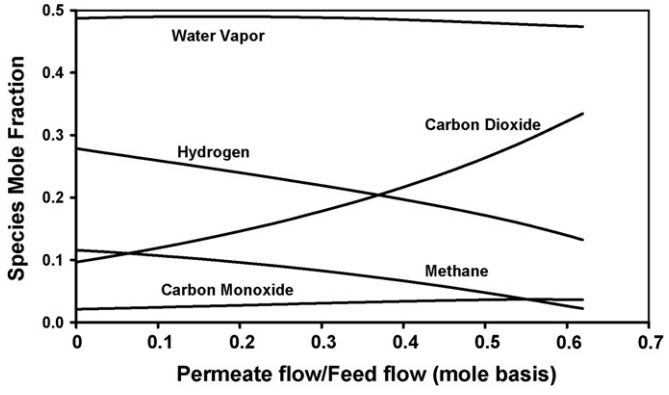


Fig. 9. Feed side gas composition, 873 K, 0.791 MPa feed side pressure, 0.101 MPa permeate side pressure, steam to carbon ratio 3.

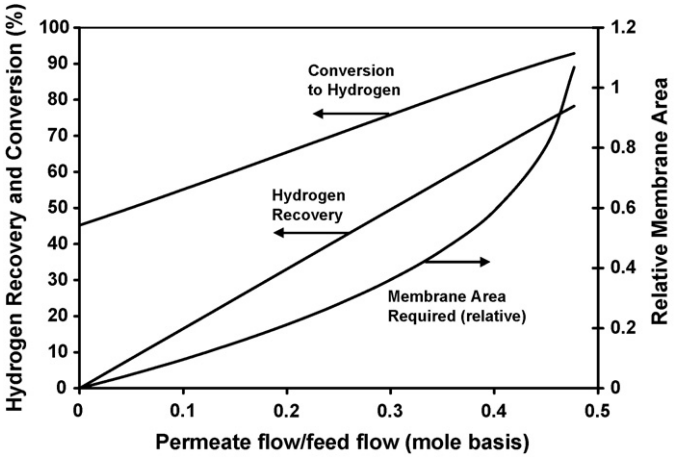


Fig. 10. Conversion of butane to hydrogen and net hydrogen recovery, at 873 K, 0.791 MPa feed side pressure, 0.101 MPa permeate side pressure, steam to carbon ratio 4.

increased conversion to hydrogen at the greater steam to carbon ratios, the net hydrogen recovery increased only modestly from 71 to 78% due to lower feed side hydrogen partial pressures and pressure gradients across the membrane that is responsible for the hydrogen recovery. The relative membrane area required to recover a unit mole of hydrogen, however, is found to be similar in all cases. Thus, utilization of a significantly greater than the

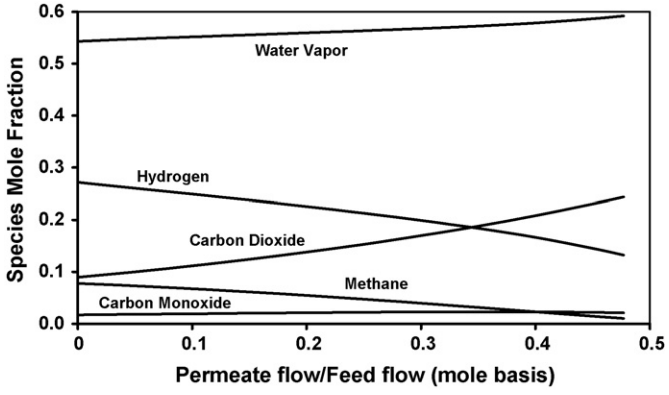


Fig. 11. Feed side gas composition, 873 K, 0.791 MPa feed side pressure, 0.101 MPa permeate side pressure, steam to carbon ratio 4.

stoichiometric steam to carbon ratio does not appear to be essential for a membrane reactor operation and similar net hydrogen recovery is predicted at stoichiometric steam to carbon ratio with similar membrane area requirements. These model simulations, however, do not include carbon formation reactions and a greater than stoichiometric steam to carbon ratio may be necessary to assure avoidance of carbon formation.

The equilibrium constant for the methanation (and the reverse methane reforming) reaction strongly depends on temperature due to the high heat of reaction. Methane reforming is favored at higher temperatures and methane formation is favored at lower temperatures. The principal hypothesis in these model simulations is that of dynamic equilibrium on the feed side at all times (i.e. faster kinetics and hydrogen generation compared to hydrogen permeation rates) which would be less true at a lower temperature compared to a higher temperature. Simulations were therefore conducted at 550 °C (823 K) as well as at 650 °C (923 K) membrane reactor operating temperatures, steam to carbon ratio of 2 and feed pressure of 100 psig (0.791 MPa) for comparison with corresponding simulations at 600 °C (873 K). The predicted hydrogen conversion and net hydrogen recovery as a function of hydrogen permeated for the membrane reactor temperature of 550 °C (823 K) are presented in Fig. 12. Comparison of Figs. 4 and 12 indicates that the net achievable hydrogen recovery is predicted to decrease substantially (from 71 to 51%) by operating the membrane reactor at 550 °C (823 K) instead of 600 °C (873 K) with otherwise similar process conditions. The reason for this decrease is that lower temperature favors methane formation and thus conversion to hydrogen is significantly decreased from 76 to 58% resulting in low initial feed side hydrogen concentrations. As a result the relative membrane area requirement is also significantly higher for operation at 550 °C (823 K). The actual area requirement will be greater still for palladium-based hydrogen separation membranes due to slightly lower permeability at the lower temperature of 550 °C (823 K) compared to that at 600 °C (873 K). Membrane reactor operation at a greater pressure of 150 psig (1.136 MPa) allows the net hydrogen recovery to increase significantly to 60% (Fig. 13) but is still much less than 76% predicted for membrane reactor operation at 600 °C (873 K) and 150 psig (1.136 MPa) feed side pressure.

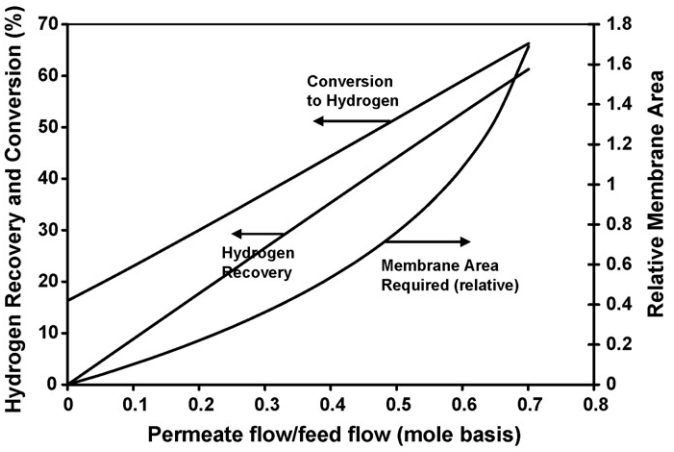


Fig. 13. Conversion of butane to hydrogen and net hydrogen recovery, at 823 K, 1.136 MPa feed side pressure, 0.101 MPa permeate side pressure, steam to carbon ratio 2.

The predicted hydrogen conversion and net hydrogen recovery as a function of hydrogen permeated for the membrane reactor temperature of 650 °C (923 K) are presented in Fig. 14. Comparison of Figs. 4 and 14 indicates that the net achievable hydrogen recovery is predicted to increase (from 70 to 78%) by operating the membrane reactor at 650 °C (923 K) with otherwise similar process conditions. The reason for this increase is that higher temperature favors methane reforming increasing conversion to hydrogen significantly from 76 to 85% resulting in greater initial feed side hydrogen concentrations. As a result the relative membrane area requirement is also significantly reduced for operation at 650 °C (923 K). As can be seen by these simulations membrane reactor operating temperature has significant impact on the equilibrium gas compositions and thus affects the membrane reactor performance. Temperature also affects material properties, seals, and membrane stability as well as permeation characteristics. Higher temperature increases

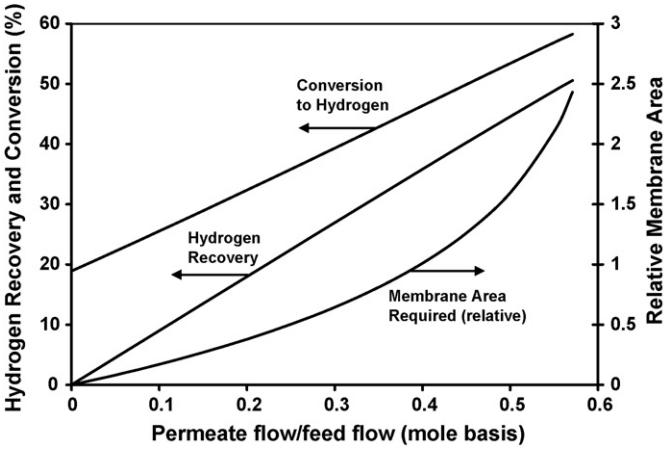


Fig. 12. Conversion of butane to hydrogen and net hydrogen recovery, at 823 K, 0.791 MPa feed side pressure, 0.101 MPa permeate side pressure, steam to carbon ratio 2.

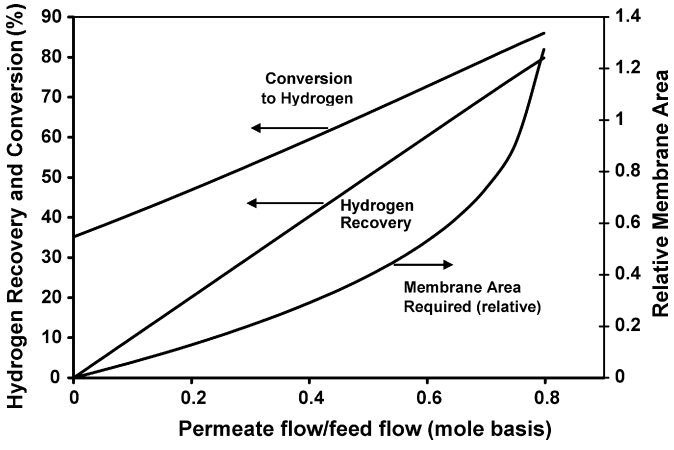


Fig. 14. Conversion of butane to hydrogen and net hydrogen recovery, at 923 K, 0.791 MPa feed side pressure, 0.101 MPa permeate side pressure, steam to carbon ratio 2.

the hydrogen permeability of the membrane but is also likely to decrease stability.

### 4.2. Methanol steam reforming

The simulation results discussed above were obtained with feed gas composition expected for the case of butane reforming. As discussed earlier, the gas composition expected with methanol reforming is only slightly different for the same equivalent steam to carbon ratio. The gas compositions expected with hydrocarbons with higher carbon number than butane will be intermediate of those with butane and methanol reforming. Simulations were therefore conducted with feed gas compositions expected with methanol reforming at 600 °C (873 K) and 100 psig (0.791 MPa) pressure and methanol to steam ratio of 1 (equivalent of steam to carbon ratio of 2 for butane reforming). The predicted hydrogen conversion and net hydrogen recovery as a function of hydrogen permeated are presented in Fig. 15.

Comparison of Figs. 4 and 15 show similar results with slightly less net hydrogen recovery with methanol reforming due to a slightly lower hydrogen concentration predicted in the feed gas. Although the model predictions based on dynamic feed side equilibrium are similar for methanol and butane reforming the kinetics of the reactions would likely be different. Methanol decomposes readily with fast kinetics at elevated temperatures with complete conversion to hydrogen and carbon monoxide (reaction (5)). Whereas, the assumption of fast kinetics may not be true for hydrocarbon reforming reaction (reaction (1)) at the lower reforming temperature of 600 °C (873 K) than typically used in commercial practice.

### 4.3. Membrane reactor operating regimes

For portable generation of hydrogen, an important consideration is to maximize the energy efficiency of the process and to obtain the maximum yield of hydrogen from the hydrocarbon being reformed. In the membrane reactor approach, the heat necessary for the endothermic hydrocarbon reforming reaction may be provided by combustion of part of the hydrocarbon fuel itself and/or by combustion of the feed side residual exhaust gases as shown in Fig. 1. Because of the requirement of a positive partial pressure differential for hydrogen permeation, the feed side exhaust gas contains significant hydrogen as well as un-reacted CO and methane. It is necessary to utilize the heat value of the membrane reject gas to provide part or all of the energy required for the hydrocarbon reforming process for increasing the overall energy efficiency of hydrogen generation. The concept of providing all of the necessary heat internally by combustion of residual exhaust gas will determine the practical hydrogen recovery achievable in a membrane reactor. Another important consideration in designing a membrane reactor process is the hydrogen partial pressure differential across the hydrogen selective membrane. By increasing hydrogen recovery the average hydrogen partial pressure across the membrane will decrease requiring greater membrane area. The incremental membrane area requirement increases dramatically at high hydrogen recoveries as more and more of hydrogen is removed as seen in the model simulation results. Both the thermal balance of the integrated system and the membrane area requirement will determine the membrane reactor operating conditions that are technically and economically feasible.

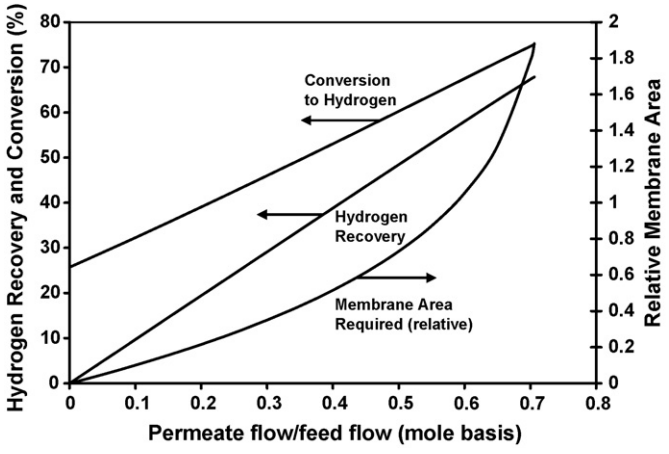


Fig. 15. Conversion of methanol to hydrogen and net hydrogen recovery, at 873 K, 0.791 MPa feed side pressure, 0.101 MPa permeate side pressure, methanol to steam ratio 1.

Hydrogen recovery increases as more and more hydrogen is produced in the permeate stream. Separating hydrogen also increases conversion of CO and methane in the feed gas to hydrogen by shifting the reaction equilibriums. The heat value of the membrane reactor feed side residual gas thus will decrease with increasing hydrogen recovery as it is depleted of hydrogen as well as of un-reacted CO and methane. The net heat requirement for the membrane reactor process for a specified hydrogen recovery is determined by:

- the heat energy required for the hydrocarbon reforming reaction (reactions (1) or (5)),
- heat generated by the water gas shift and methanation reactions (reactions (2) and (3)),
- heat required to vaporize and preheat fuel and water feed to the membrane reactor temperature,
- heat required to preheat the combustion air to the membrane reactor temperature,
- the heat produced by combustion of the residual gas at the membrane reactor temperature, and
- efficiency of recovering heat from the combustion of the residual gas in the integrated membrane reactor as well as the efficiency of heat exchangers used for recovery of heat from the combustor exhaust gas by heating fuel/water and air streams. Although the product hydrogen exiting membrane reactor has some heat value it is generally not significant to warrant a dedicated heat exchanger [25]. Depending on the water vapor content of the exit residual gas, the residual gas may first be cooled to remove water before the combustion of the residual gas.
- loss of heat energy from the entire system to ambient.

The net heat requirement/availability for a given hydrogen recovery may be estimated assuming an overall heat recov-

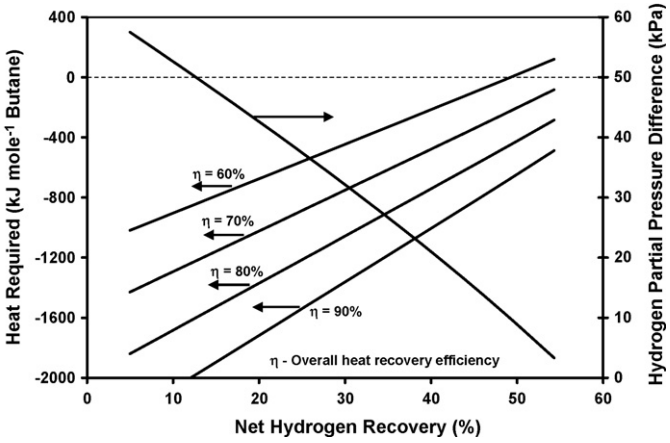


Fig. 16. Net heat required and hydrogen partial pressure differential, membrane reactor at 873 K, 0.515 MPa feed side pressure, 0.101 MPa permeate side pressure, steam to carbon ratio 2.

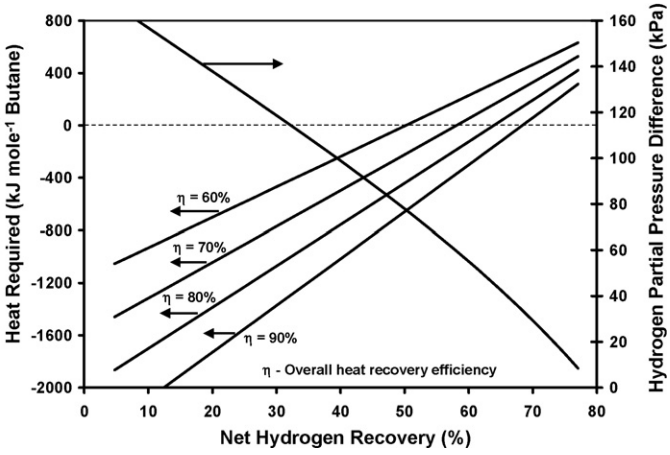


Fig. 18. Net heat required and hydrogen partial pressure differential, membrane reactor at 873 K, 1.136 MPa feed side pressure, 0.101 MPa permeate side pressure, steam to carbon ratio 2.

ery efficiency to account for the individual combustor and heat exchanger efficiencies, intermediate residual gas cooling if used, as well as the heat losses from the entire system. The hydrogen partial pressure differential at the membrane reactor outlet conditions is determined by the mole fraction of hydrogen and the operating pressure in both the feed and permeate streams at the reactor outlet conditions. For an efficient membrane reactor system for hydrogen generation, the hydrogen recovery should be chosen such that the system produces a small net heat rejected to the ambient and the hydrogen partial pressure differential at the reactor exit remains above a certain threshold value to avoid excessive membrane area requirement. Depending upon the process parameters either the net heat criterion or the hydrogen driving force criterion will determine the achievable hydrogen recovery for those process conditions.

Figs. 16–18 provide the net heat required/produced in the membrane reactor as well as the hydrogen partial pressure differential across the membrane as a function of net hydrogen recovery and an overall efficiency of heat recovery again for the cases of steam reforming of butane at 600 °C (873 K), stoichiometric steam to carbon ratio of 2, and feed gas pressures of 60, 100, and 150 psig (0.515, 0.791, and 1.136 MPa), respectively. The net heat requirement is expressed as that calculated for the basis of one mole of butane feed to the membrane reactor and is calculated for overall heat recovery efficiencies of 60, 70, 80, and 90%, respectively. A negative value for the net heat requirement indicates that a net heat is produced in the membrane reactor. The net heat required/produced takes into account the reaction heats of all of the reactions, heat generated by combustion of the residual gases, heat required for heating the reagents (butane and water) as well as the combustion air to the membrane reactor conditions, and the heat recovered from exhaust combustion gases.

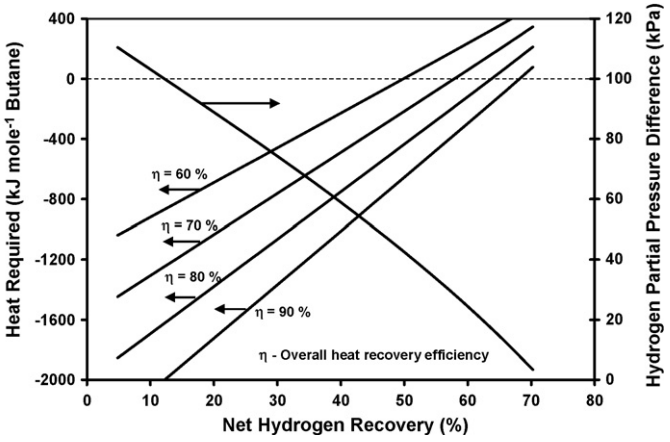


Fig. 17. Net heat required and hydrogen partial pressure differential, membrane reactor at 873 K, 0.791 MPa feed side pressure, 0.101 MPa permeate side pressure, steam to carbon ratio 2.

As seen from these figures the overall efficiency of heat recovery from residual gas strongly determines the practical hydrogen recoveries that can be achieved. Although greater net hydrogen recoveries are possible by membrane reactor operation at higher pressures, the practical hydrogen recovery as determined by the thermal balance remains the same for a given heat recovery efficiency as expected regardless of system pressure. For reforming of butane at 600 °C (873 K), stoichiometric steam to carbon ratio of 2, and an overall heat recovery efficiency of 90%, the achievable hydrogen recovery is about 68% to assure generation of sufficient heat internally, i.e. by combustion of the residual gas to generate all the required heat for the reforming process as well as for heating all feed streams. Operation at higher pressures obviously will reduce the membrane area requirement, e.g. comparison of Figs. 4 and 5 indicate that operation of the membrane reactor at 100 psig (0.791 MPa) will require almost 60% more membrane area than that for 150 psig (1.136 MPa) operation for the same 68% net hydrogen recovery. For reforming of butane at the lower pressure of 60 psig (0.515 MPa), at 600 °C (873 K) reactor temperature, the net hydrogen recovery is limited to only 55% regardless of the heat recovery efficiency by the requirement of maintaining sufficient hydrogen partial pressure differential (e.g. ~0.5 psia (3347 Pa) as used in the model simulations) across the membrane. Utilization of greater membrane reactor operating pressure will require a higher pressure

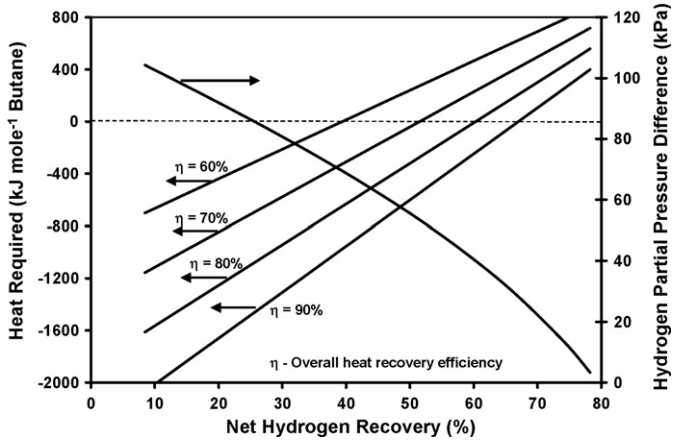


Fig. 19. Net heat required and hydrogen partial pressure differential, membrane reactor at 873 K, 0.791 MPa feed side pressure, 0.101 MPa permeate side pressure, steam to carbon ratio 4.

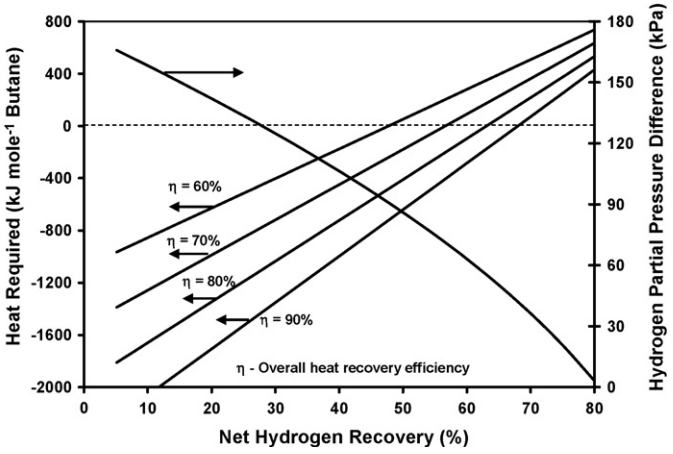


Fig. 21. Net heat required and hydrogen partial pressure differential, membrane reactor at 923 K, 0.791 MPa feed side pressure, 0.101 MPa permeate side pressure, steam to carbon ratio 2.

pump and additional power for the pump operation that is not accounted for in the energy balance calculations. Membrane reactor operation at greater steam to carbon ratio allows greater butane conversion to hydrogen as seen in Figs. 8 and 10, for steam to carbon ratios of 3 and 4, respectively, but it also requires greater energy for steam generation and the practical achievable hydrogen recovery is slightly less than that for membrane reactor operation at stoichiometric steam to carbon ratio for the same overall heat recovery efficiency as seen in Fig. 19 for steam to carbon ratio of 4. Comparison of Figs. 4 and 10 indicate that the membrane area required for recovery of the same amount of hydrogen is only slightly greater for the stoichiometric steam operation. A greater steam to carbon ratio will require additional weight of water reducing the energy density of the overall system. Operation of the membrane reactor at stoichiometric steam to carbon ratio will thus maximize the energy density of the overall system.

The net heat requirement for butane reforming at 550 °C/150 psig (823 K/1.136 MPa) and at 650 °C/100 psig (923 K/0.791 MPa) process conditions are shown in Figs. 20 and 21, respectively. The achievable hydrogen recovery at 650 °C (923 K) is similar to that for 600 °C (873 K) temperature of about 68% with overall heat recovery efficiency of 90%. At the lower temperature of 550 °C (823 K), however, the hydrogen recovery is limited to about 63% due to the positive partial pressure differential requirement even at the high operating pressure of 150 psig (1.136 MPa) with 90% efficiency for heat recovery.

For the cases of steam reforming of methanol at 600 °C (873 K), steam to methanol ratio of 1, and feed gas pressures of 100 and 150 psig (0.791 and 1.136 MPa), the net heat requirement for the membrane reactor as well as the hydrogen partial pressure differential as a function of net hydrogen recovery, are presented in Figs. 22 and 23, respectively. Due to the lower reaction heat requirement for methanol reforming, up to 76% net hydrogen recovery is possible at 150 psig (1.136 MPa) pressure operation with an overall heat recovery efficiency of 90% while providing all of heat requirement internally as seen in Fig. 23. At the lower 100 psig (0.791 MPa) pressure operation, however, the net hydrogen recovery is limited to 67% by the requirement of maintain-

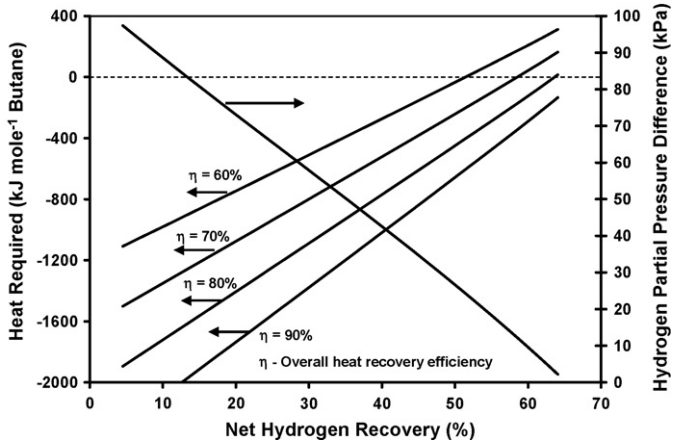


Fig. 20. Net heat required and hydrogen partial pressure differential, membrane reactor at 823 K, 1.136 MPa feed side pressure, 0.101 MPa permeate side pressure, steam to carbon ratio 2.

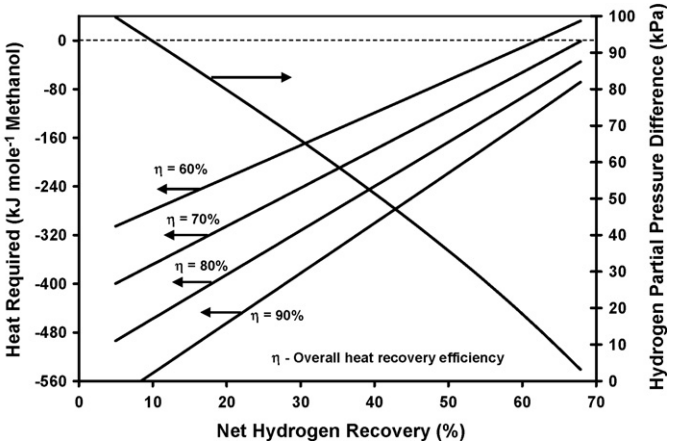


Fig. 22. Net heat required and hydrogen partial pressure differential, membrane reactor at 873 K, 0.791 MPa feed side pressure, 0.101 MPa permeate side pressure, steam to methanol ratio 1.

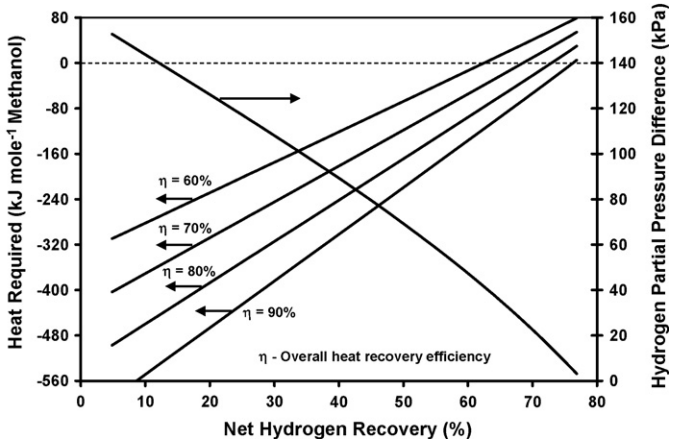


Fig. 23. Net heat required and hydrogen partial pressure differential, membrane reactor at 873 K, 1.136 MPa feed side pressure, 0.101 MPa permeate side pressure, steam to methanol ratio 1.

ing sufficient hydrogen partial pressure differential across the membrane.

In general, these simulations indicate that the practical achievable net hydrogen recovery in a thermally integrated membrane reactor for steam reforming of butane at 600 °C (873 K) is about 68%, assuming an overall heat recovery efficiency of 90%, almost independent of the system pressure or steam to carbon ratio. Due to lower heat requirement for methanol reforming, up to 76% hydrogen recovery is achievable with membrane reactor feed side pressure of 150 psig (1.136 MPa). In general, for operation at lower pressures (e.g. 60 psig (0.515 MPa) for butane reforming and 100 psig (0.791 MPa) for methanol reforming) the achievable hydrogen recovery is limited by the requirement of maintaining sufficient hydrogen partial pressure differential at the membrane reactor exit conditions. Higher pressure operation will reduce the required membrane area however will require appropriate high pressure pumps for supplying butane and water reagents. Availability and weight of the high pressure pump will determine the maximum pressure that can be practically used. The hydrogen permeation characteristics of the hydrogen selective membrane will determine the actual membrane area required. For portable power generation application, the overall size and weight of the membrane reactor as well as the balance of plant components such as high pressure pump, blower for combustion air and heat exchangers are also important for optimal selection of membrane reactor operating conditions.

## 5. Membrane reactor design

The model simulations presented here assume dynamic reaction equilibrium on the feed side of the membrane reactor at all times. In practice, the reaction kinetics or the chemical conversion actually achieved depends on the membrane reactor temperature, pressure, catalysts used, and the residence time (space velocity) of the feed gas through the catalyst. Simultaneous hydrocarbon reforming, methanation/methane reforming and WGS reactions (reactions (1)–(3)) are involved in determining net hydrogen generation rate in the membrane reactor. For an optimal membrane reactor design there should be a good match between the rate of hydrogen generation on the feed side and the rate of hydrogen permeation by membrane. The extent of reaction or hydrogen generation depends on the rate of reaction at the prevailing process operating conditions, species concentrations, catalyst used and its effectiveness, and the volume of the feed side catalyst zone. The rate of hydrogen removal depends on the permeation characteristics of the membrane, hydrogen partial pressure differential across the membrane, and the available membrane surface area.

The results of model simulations discussed here provide an insight in to the effect of hydrogen removal on the possible extent of reaction conversion to hydrogen and possible hydrogen recovery at various process conditions used. The rate of reactions must be determined experimentally for the specific catalyst used at the process conditions of temperature, pressure, and space velocity of interest. Hydrogen generation by steam reforming of butane, methanol, and clearlite in a membrane reactor was experimentally evaluated using commercially available Pd–Ag alloy foils as hydrogen separation membrane. The experimental results are compared with model predictions in the companion paper.

To maximize total system-based specific energy, weight of all other system components (besides the hydrocarbon fuel) must be minimized in every way possible. Since heat is required to release hydrogen from these fuels, efficient utilization of thermal energy is necessary. Hydrocarbon reforming must also overcome additional challenges: carbon formation/coking during hydrocarbon reforming process and resulting deactivation of catalysts, sensitivity of catalysts to even small traces of sulfur in fuel, and removal of carbon monoxide from the product hydrogen. The model simulations thus provide estimates of maximum possible hydrogen recoveries at different process operating conditions and the extent of heat recovery from exhaust streams in the membrane reactor configuration.

## 6. Summary and conclusions

PEM fuel cells provide an attractive option for lightweight, compact, portable power generation. PEM fuel cells, however, require a source of pure hydrogen. Reforming of liquid hydrocarbon fuels is most promising for providing high reagent weight-based hydrogen generation and specific energy; greater than 2 kWh $kg^{-1}$ including weight of water. Commonly available liquid hydrocarbon fuels such as butane also possess desirable characteristics such as ease of fuel storage at low pressures and ambient temperatures, handling and transportation; availability, and a low cost. Steam reforming of hydrocarbons produces hydrogen in equilibrium limited reactions conducted at high pressures and temperatures. Utilization of a membrane reactor with a high temperature hydrogen permeable membrane such as Pd-alloy membrane, overcomes the equilibrium limitation of the reforming and WGS reactions as well as allow conducting these reactions under milder conditions. Integration of the fuel reforming, hydrogen separation, and the fuel combustion section to provide the necessary heat for reactions allows producing hydrogen in a compact efficient portable system. Optimization of the system temperature, pressure and operating

parameters such as steam to carbon ratio and hydrogen recovery is necessary to realize an efficient integrated membrane reformer suitable for compact portable hydrogen generation. Simulation of the integrated membrane reactor/reformer operation was conducted using a simple theoretical model of the process to determine the effect of operating parameters of temperature, feed side pressure, and steam to carbon ratio on the extent of fuel conversion to hydrogen and hydrogen recovery in the permeate product.

In a membrane reformer operation, utilization of thermal energy is maximized by using the heat value of the membrane reject gas to provide all of the heat necessary for the reforming reactions. The maximum achievable hydrogen recovery in a membrane reformer is thus limited by the need to maintain positive hydrogen partial pressure differential across the membrane as well as by the need to retain sufficient heat value in the membrane reject gas. Model simulations indicated that the hydrogen recovery is limited to 68% of the maximum possible when butane is used as a fuel with an overall heat recovery efficiency of 90%. Membrane reformer operation at 600 °C (873 K) temperature and 100 psig (0.791 MPa) pressure, process conditions milder than conventional methane reforming, is able to achieve the optimal hydrogen recovery. Operation at a greater pressure or temperature was predicted to provide marginal improvement in the performance whereas operation at a lower temperature or pressure was predicted to be unable to achieve the optimal performance. Higher hydrogen recovery of up to 76% is possible when methanol is used as a fuel at 150 psig (1.136 MPa) feed pressure and 600 °C (873 K) temperature due to the lower heat requirement for methanol reforming reaction. When operated at 100 psig (0.791 MPa) pressure, however, the hydrogen recovery for methanol reforming was limited to 67% by the requirement of maintaining positive hydrogen partial pressure differential across the membrane.

## Acknowledgement

Partial support for this work by Defense Advanced Research Projects Agency (DARPA) (research contract #DAAD19-01-C-0069) is gratefully acknowledged.

## References

[1] A.S. Patil, T.G. Dubois, N. Sifer, E. Bostic, K. Gardner, M. Quah, C. Bolton, J. Power Sources 136 (2004) 220–225.
[2] S. Ahmed, J. Kopasz, R. Kumar, M. Krumpelt, J. Power Sources 112 (2002) 519–530.
[3] J.D. Holladay, E.O. Jones, R.A. Dagle, G.G. Xia, C. Cao, Y. Wang, in: Y. Wang, J.D. Holladay (Eds.), Microreactor Technology and Process Intensification, ACS Symposium Series 914, American Chemical Society, Washington, DC, 2005, pp. 162–178.
[4] J.R. Rostrup-Nielsen, in: J.R. Anderson, M. Boudart (Eds.), Catalysis, Science and Technology, Springer-Verlag, New York, 1984.
[5] S. Roychoudhary, M. Castaldi, M. Lyubovsky, M.R. LaPierre, S. Ahmed, J. Power Sources 152 (2005) 75–86.
[6] Q. Ming, A. Lee, J. Harrison, P. Irving, in: Y. Wang, J.D. Holladay (Eds.), Microreactor Technology and Process Intensification, ACS Symposium Series 914, American Chemical Society, Washington, DC, 2005, pp. 224–237.
[7] D.R. Palo, J.D. Holladay, R.A. Dagle, Y.H. Chin, in: Y. Wang, J.D. Holladay (Eds.), Microreactor Technology and Process Intensification, ACS Symposium Series 914, American Chemical Society, Washington, DC, 2005, pp. 209–223.
[8] A. Criscuoli, A. Basile, E. Drioli, O. Loiacono, J. Membr. Sci. 181 (2001) 21–27.
[9] Y.M. Lin, M.H. Rei, Catal. Today 67 (2001) 77–84.
[10] A. Basile, G. Chiappetta, S. Tosti, V. Violante, Sep. Purif. Technol. 25 (2001) 549–571.
[11] J. Shu, B.P.A. Grandjean, S. Kaliaguine, Appl. Catal. A: Gen. 119 (1994) 305–325.
[12] S. Uemiya, N. Sato, H. Ando, T. Matsuda, E. Kikuchi, Appl. Catal. 67 (1991) 223–230.
[13] IdaTech, Fuel Processing Technology and ElectraGen product information available at http://www.idatech.com/technology/fuel_processors.html and http://www.idatech.com/media/pdf/ElectraGen_XTRModule.pdf (accessed October 2007).
[14] InnovaTek, InnovaGen Fuel Processor product information available at http://www.tekkie.com/docs/InnovaGen.pdf (accessed October 2007).
[15] Intelligent Energy, Fuel Processor and hydrogen generator product information available at http://www.intelligent-energy.com/images/uploads/compact_hydrogen_generator_a4.pdf (accessed October 2007).
[16] R. Dittmeyer, V. Hollein, K. Daub, J. Mol. Catal. A: Chem. 173 (2001) 135–184.
[17] H. Amandusson, L.G. Ekedahl, H. Dannetun, J. Catal. 195 (2000) 376–382.
[18] H. Nagamoto, H. Inoue, Chem. Eng. Commun. 34 (1985) 315–323.
[19] N. Itoh, AIChE J. 33 (1987) 1576–1578.
[20] J.A. Bitter, Brit. Patent G. B. 2,201,159,24 (1988).
[21] A.S. Damle, S.K. Gangwal, V.K. Venkataraman, Gas Sep. Purif. 8 (1994) 101–106.
[22] T.L. Ward, T. Dao, J. Membr. Sci. 153 (1999) 211.
[23] S.N. Paglieri, J.D. Way, Sep. Purif. Methods 31 (2002) 1–169.
[24] HSC Chemistry, Outokumpu HSC Chemistry for Windows, Version 4.0, Outokumpu Research, June 1999.
[25] A. Chellappa, Intelligent Energy, Albuquerque, New Mexico, Personal communications, September 2007.